

Microstructure and magnetic properties of electrodeposited cobalt films

M. S. Bhuiyan · B. J. Taylor · M. Paranthaman ·
J. R. Thompson · J. W. Sinclair

Received: 7 September 2007 / Accepted: 4 December 2007 / Published online: 11 January 2008
© Springer Science+Business Media, LLC 2008

Abstract Cobalt films were electrodeposited onto both iron and copper substrates from an aqueous solution containing a mixture of cobalt sulfate, boric acid, sodium citrate, and vanadyl sulfate. The structural, intermetallic diffusion and magnetic properties of the electrodeposited films were studied. Cobalt electrodeposition was carried out in a passively divided cell aided by addition of vanadyl sulfate to keep the counter electrode clean. The divided electrolytic cell with very negative current densities cause the electrodeposited Co to adopt a face-centered cubic (fcc) structure, which is more magnetically reversible than the hexagonally close-packed (hcp) structured Co. The coercive field is also significantly less in the fcc-electrodeposited cobalt than in the hcp. SEM images show dense, uniform Co films without any cracks or porosity. Beside the deposition current, thickness of the film was also found to affect the crystal orientation particularly on iron substrates. Diffusion of cobalt film into the iron substrate was studied under reduced environment and a fast process was observed.

Introduction

The increasing demand in the design of transformers, motors, and generators for use in electric vehicles and other high-temperature applications has triggered intensive investigations of alloys of iron groups that exhibit high-saturation magnetization M_s and high Curie temperatures T_c ($T_c \sim 900$ °C) [1–6]. Cobalt and cobalt alloys have magnetic and electrical properties that are very attractive for technological applications such as magnetic recording, transformer core materials, thin film inductors, and giant magneto-impedance sensors [7–10]. Electrochemical deposition of cobalt has been carried out on substrates such as nickel, vitreous carbon, and copper, and from different electrolytic baths containing chloride, sulfate, or thiocyanate aqueous solutions [11–14]. However, reports on cobalt electrodeposition on iron substrates have yet to define the mechanisms involved. Though codeposition of Co–Fe alloys has been performed successfully [7], from the applications point of view growth of Co film on Fe substrates is preferable. It is well known that Fe and Co form body-centered cubic (bcc) solid solution ($\text{Co}_x\text{Fe}_{100-x}$) over an extensive range [15]. In the range of $30 < x < 70$, FeCo alloys undergo a phase transformation from a disordered bcc structure to the ordered CsCl type structure below 730 °C [16]. The ordered FeCo alloys are excellent soft magnetic materials with negligible magneto-crystalline anisotropy K_1 [17]. However, the equiatomic FeCo alloys are extremely brittle and other elements such as V are usually added to obtain workable materials. The brittle nature of FeCo binary alloys is attributed to the formation of an ordered $B2/L2_o$ superlattice from the bcc solid solution below 730 °C. Additional elements such as V induce precipitation of a second phase of $L1_2$ structure [18, 19], whose volume percent and morphology depend on the

M. S. Bhuiyan · B. J. Taylor · M. Paranthaman (✉)
Materials Chemistry Group, Chemical Science Division,
Oak Ridge National Laboratory, Oak Ridge, TN 37831, USA
e-mail: paranthamanm@ornl.gov

B. J. Taylor
Tennessee Technological University, Cookeville, TN 38505,
USA

J. R. Thompson
Materials Science and Technology Division, Oak Ridge National
Laboratory, Oak Ridge, TN 37831, USA

J. R. Thompson · J. W. Sinclair
Department of Physics, University of Tennessee, Knoxville,
TN 37996-1200, USA

concentration of the added elements. The precipitation of second phase, however, significantly deteriorates the soft magnetic properties [20]. Besides the second phase, all other structural defects such as grain boundaries [6] and dislocations also considerably affect the magnetic properties especially the coercive field, H_c . However, we believe that instead of equiatomic FeCo alloys, deposited Co film can be diffused into the Fe substrate to make Co-deficient FeCo alloys without V addition for the electrical equipment applications.

Since the electrodeposition technique is a very promising candidate to produce Co films on Cu and Fe substrates with quality competitive with those produced by physical vapor deposition (PVD) techniques, we have chosen electroplating technique for cobalt film growth and characterization of these films. In this article, we report a comprehensive and systematic study to understand the growth process, effects of control parameters on structure and microstructure, and microstructural dependence on the film thickness. Also the effects on the magnetic and structural properties of Co were investigated by electrodeposition of Co film on Cu substrates.

Experimental

All deposition experiments were performed using a stationary passively divided electrode system consisting of a Pt counterelectrode surrounding the central working electrode with a separating membrane. Both plate (0.1 mm thickness) and wire (0.5 mm diameter) of Fe and Cu were used as the working electrodes. Co films were grown on slightly (2 0 0) textured polycrystalline Fe and Cu plates washed with deionized water, cleaned with acetone by ultrasonic process, and rinsed with deionized water before being placed in the electrolyte. To simplify magnetic measurements, Co film was deposited on Cu round wire. Diffusion of cobalt into iron was tested by depositing Co on both Fe tapes and wires. A Princeton Applied Research potentiostat/galvanostat (Model 173) was used to control the applied current during the depositions with a Princeton Applied Research Digital Coulometer. All depositions were performed under constant current condition. Deposition rate and film thickness were controlled by varying applied current and deposition time. The thickness uniformity of the electrodeposited films was determined by using a stylus profiler.

The plating bath was prepared by dissolving 0.5 M cobalt sulfate, 0.1 M vanadyl sulfate, 0.1 M boric acid, and 0.1 M sodium citrate in deionized water. All chemical reagents used were as received from Alfa Aesar. Deaeration of the electrolyte solutions was not performed. The constant current mode electrodeposition of cobalt was

carried out at room temperature with 0.5 M cobalt solution prepared as described with the presence of boric acid and sodium citrate as additives for the pH adjustment in the range of 2–3. A moderate agitation was maintained by stirring at the rate of 300–500 rpm during the deposition to help remove the bubbles from the electrode surfaces. All the electrodeposition experiments were carried out at room temperature with the variation of solution pH, current density, and time. The nominal current densities were obtained through direct division of cathodic current by geometrical area of the working electrode.

The electroplated samples were characterized using X-ray diffraction (XRD), scanning electron microscopy (SEM), and SQUID magnetometry. Surface characterization of the metallic coating was obtained by XRD using a Rigaku Rotaflex diffractometer using Cu-K α radiation and power rating of 50 kV and 100 mA. The morphology and microstructure of the cobalt films were determined by SEM analyses using a Hitachi S-4100 field emission SEM. For magnetic measurements, cobalt-coated Cu wires were cut into strips of about 6 mm in length and mounted between two plastic tubes such that the long axis of the wire was parallel to the magnetic field in a SQUID-based magnetometer. The magnetic moment m was measured as a function of applied magnetic field in the range from 0 Oe to 65,000 Oe and then from 65,000 Oe to -500 Oe. Measurements were conducted at temperatures of 5 K and then from 50 K to 300 K in 50 K steps.

Results and discussion

Cobalt deposition on copper substrate

Copper tapes with dimension 5 mm \times 40 mm (width \times length) were electrochemically deposited under the conditions described above. The effective deposition length is between 20 mm and 30 mm. X-ray diffraction analysis shows that electrodeposited Co favors hexagonally close-packed (hcp) structure at lower negative current densities (2–40 mA/cm²), face-centered cubic (fcc) structure at higher negative current densities (150 + mA/cm²), and mixed phases of fcc and hcp in between. Figure 1 shows the XRD patterns for three different cobalt films on copper substrates deposited with current densities 13.5, 74, and 154 mA/cm², respectively, as presented from bottom to top in the graph. The bottom pattern is consistent with hcp-structured cobalt, middle is the mixed phase of hcp and fcc, and the top one purely fcc structure. Control of crystal structure is very important for tuning magnetic properties in the cobalt. Here we have demonstrated that the crystal structure, particularly on copper substrates, can be tuned by controlling the deposition parameters. The structural

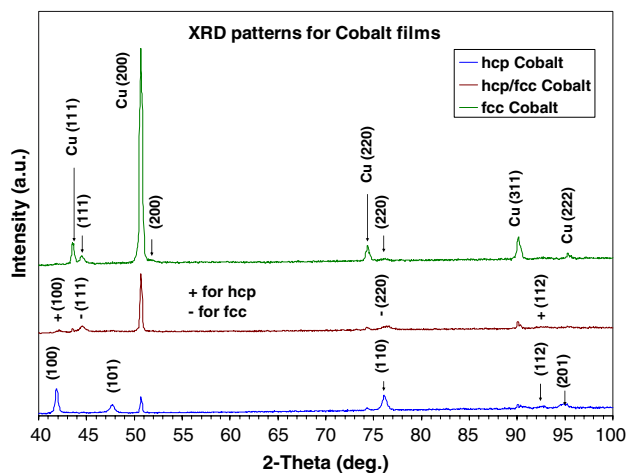


Fig. 1 An XRD plot for cobalt films grown on copper substrates using electrochemical deposition

variation with current density is also evident from the SEM images. Figure 2 shows the surface morphology of two films deposited at 13.5 and 153.5 mA/cm² current density.

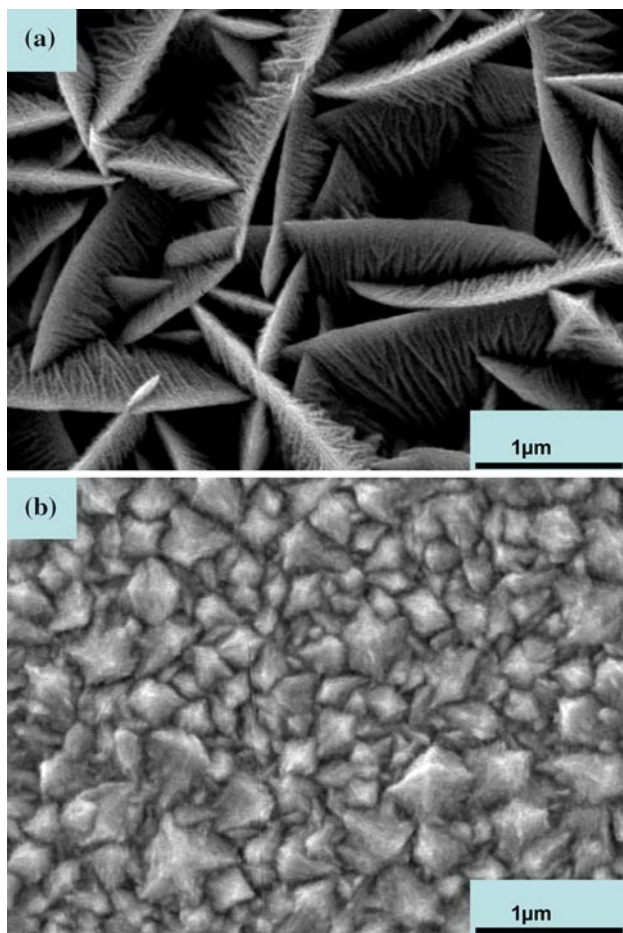


Fig. 2 SEM micrographs of cobalt film on copper substrates for (a) low current density and (b) high current density deposition

Samples created under low current density formed nanocomb grains (Fig. 2a), while samples prepared under high current density formed pyramidal structures (Fig. 2b). At this point it is not clear how these two very different structures evolve. Further experimental analysis is necessary to fully understand this interesting behavior of the cobalt film on copper substrates.

The magnetic response of samples electrodeposited in fcc and hcp orientations, corresponding to very high negative current and very low negative current, respectively, is shown in Fig. 3. The saturation magnetic moment m_{sat} (at $T = 5$ K) was 8.66 and 10.1 millimu for the two respective cases (1 millimu = 10^{-3} G cm³). Assuming that the saturation magnetization (magnetic moment/volume) is that of bulk cobalt metal, $M_{\text{sat}} = 1,446$ G, we determined the volume of cobalt and normalized M accordingly. (Note that M_{sat} is very nearly the same for hcp and fcc forms of cobalt.) Values for the corresponding thickness of the electrodeposited films are 0.328 μm and 0.389 μm . The more interesting effect was seen in the cobalt film deposited with very high negative current. The resulting fcc cobalt film exhibits a significantly reduced magnetic hysteresis, compared with the hcp film. This is dramatically evident in the coercive field, H_c of the fcc-structured cobalt film. Figure 4, which presents the H_c values versus temperature for both hcp- and fcc-structured films, clearly shows that H_c is significantly reduced by a factor of 6 or 7 when compared with hcp case. These results are consistent with the general trend that the magnetocrystalline anisotropy constant is lower in cubic structures than in hexagonal or lower symmetries. The so-called remnant moment, M_r of the fcc cobalt is larger than that for the hcp film (Fig. 5). Here the remnant moment was normalized by the saturation moment to eliminate the volume dependence.

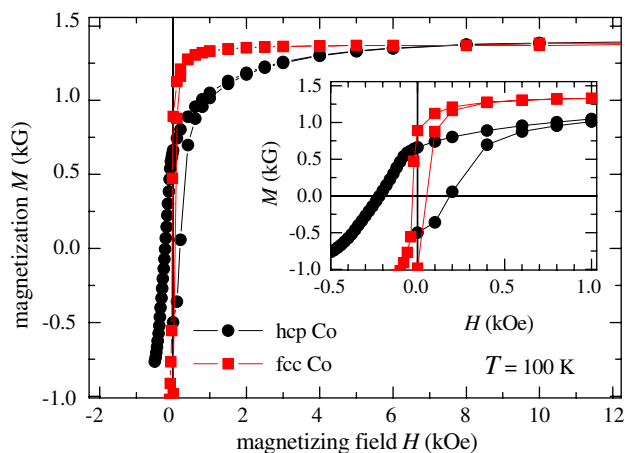


Fig. 3 Hysteresis loop for cobalt deposited on copper wire. Here H is the applied field measured in Oe (oersted) while M is the magnetic moment/volume of the sample measured in G (gauss). Inset: expanded view near the origin

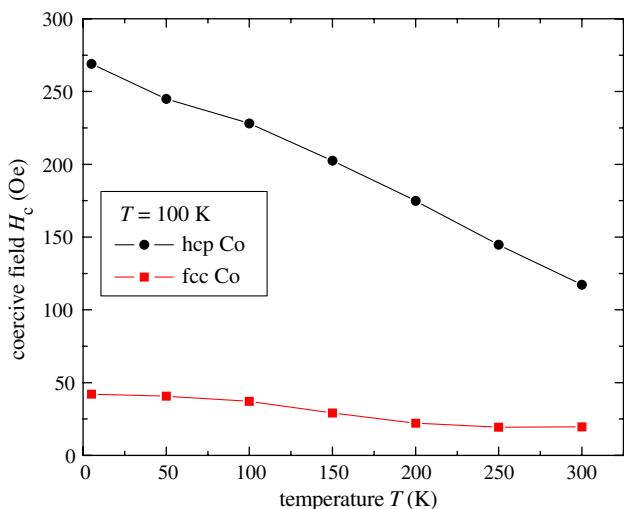


Fig. 4 A plot of the coercive field against temperature

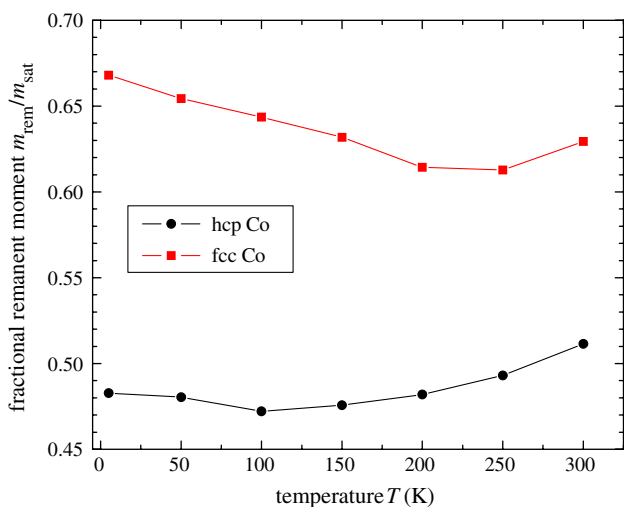


Fig. 5 The remanent moment expressed as a fraction of the saturation moment, plotted versus temperature

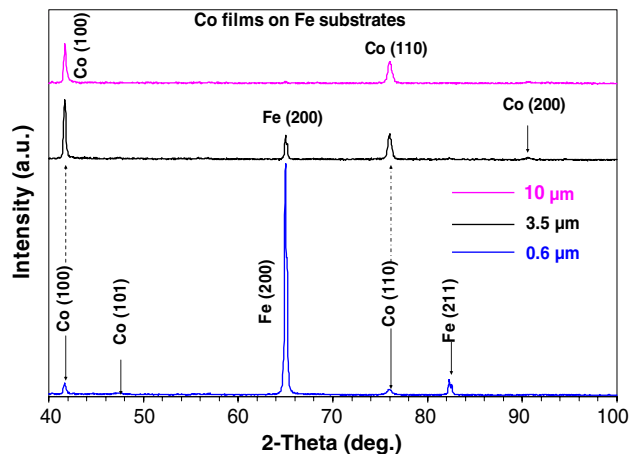


Fig. 6 Room temperature XRD patterns for cobalt films grown on iron substrates using electrochemical deposition

Cobalt deposition on iron substrate

Flat iron substrates with dimension 5 mm × 60 mm (width × length) were electrochemically deposited under constant current density condition ranging between 5 mA/cm² and 20 mA/cm². The deposited thickness was varied from 0.5 μm to 10 μm by controlling current density and deposition time. Room temperature XRD patterns for Co films on Fe substrates with three different thicknesses are shown in Fig. 6. Clearly, all these films have hcp crystal structure. It can be also noticed that the peak intensity of the Fe substrates diminishes with increase in thickness of Co.

A clear trend of Co grain orientation with the film thickness was observed. It can be seen in Fig. 7 that cobalt film with thickness 0.6 μm (Fig. 7a) has randomly oriented grain. However, as the thickness increases to 3.5 μm the grains (Fig. 7b) become oriented along *a*-axis which is parallel to the substrate surface. With further increase in

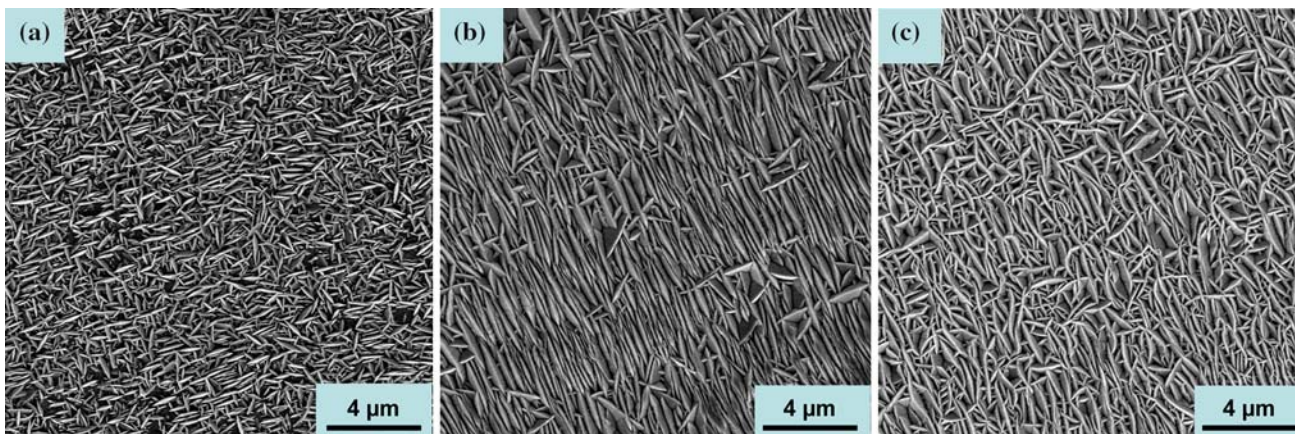


Fig. 7 Surface morphology of cobalt films with thickness (a) 0.6 μm, (b) 3.5 μm, and (c) 10 μm deposited on iron substrates

thickness (10 μm) Co film grains gradually lose this ordered form as seen in Fig. 7c. One of the obvious measure of degree of orientation is the intensity ratio of (1 0 0) peak compared to (1 1 0) peak of the Co films and clearly this value is much higher for film with thickness 3.5 μm . At this point the driving mechanism for the ordered grain cobalt film is not clear. A further investigation is important to understand the ordering of Co grain on iron substrates.

The diffusion of cobalt film into iron substrate was investigated by heat treating the Co films at 950 $^{\circ}\text{C}$ in the reducing atmosphere of Ar-4% H_2 . Both flat substrate and round wire of Fe substrate was used for this investigation. It was found that Co film (thickness of less than 5 μm) was completely miscible with Fe and formed an alloy when heat treated at 950 $^{\circ}\text{C}$ for 30 min. The samples were analyzed by XRD, AUGER, and SEM to determine if there is a presence of Co on the substrate surface after post-annealing. As per Fig. 8, X-ray reflections from pure Co film were absent possibly due to the complete miscibility of Co into Fe. There was no noticeable shift in the Fe reflection observed. This could be mainly due to the low content of Co present. Also, the microstructure of Co grains changed after post-annealing (see Fig. 9). To quantify the amount of Co present at the alloy surface, Auger scans were conducted on both as-prepared and post-annealed samples. Auger scans (as shown in Fig. 10) indicated the presence of Co to be around 59% at the surface after post-annealing.

Summary

We have successfully demonstrated the growth of cobalt film on both copper and iron substrates. We have also identified the electrodeposition conditions to preferentially deposit hcp, fcc, or mixed phases of cobalt film on copper

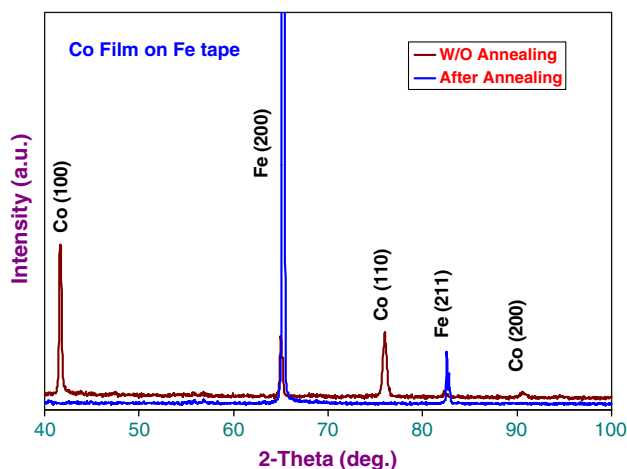


Fig. 8 Room temperature XRD patterns for both as-deposited and post-annealed (950 $^{\circ}\text{C}$; 30 min) cobalt films grown on iron substrates

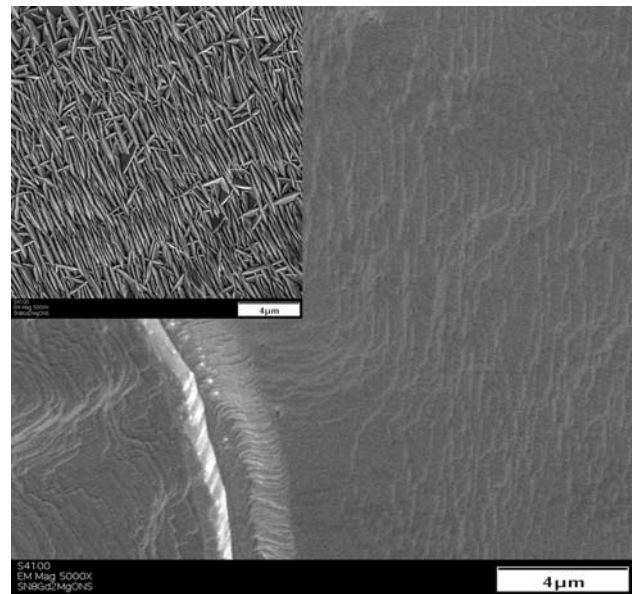


Fig. 9 SEM micrograph for the post-annealed cobalt films on iron substrates. Figure inset shows the microstructure of as-deposited cobalt films

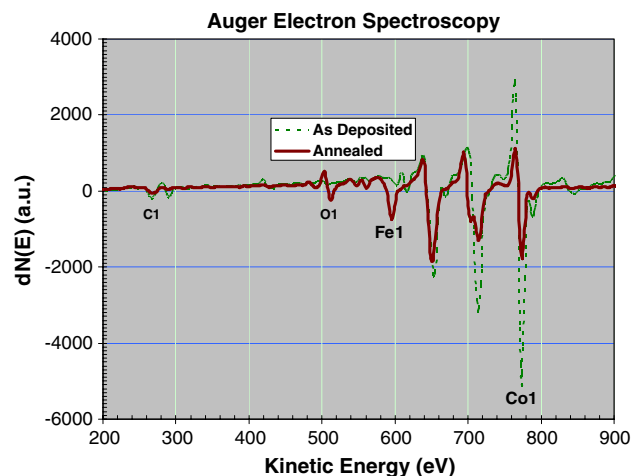


Fig. 10 AUGER depth profile scans (derivative form) of both as-deposited and post-annealed (950 $^{\circ}\text{C}$; 30 min) cobalt films grown on iron substrates

substrates. At low current density (2–40 A/cm^2), the Co film adopts an hcp structure. However, at high current density (150+ A/cm^2), the structure is mostly fcc; and in-between the current density, films with mixed hcp and fcc structures were obtained. From the magnetic measurement it was found that the coercive field is significantly lower in the fcc-electrodeposited cobalt than in the hcp. The thickness of the film has a growth effect on the orientation of cobalt film when deposited on iron substrates. More investigation is necessary to understand this behavior of grain ordering.

Acknowledgements The authors would like to thank Rad Radhakrishnan for helpful discussions and Lee Heatherly for Auger analysis. Also, thanks go to ORISE and HTML Share facilities. This work was sponsored by the Department of Energy, Office of Basic Energy Sciences—Division of Materials Sciences and Engineering, Office of Electricity Delivery and Energy Reliability (OE). This research was performed at the Oak Ridge National Laboratory, managed by UT-Battelle, LLC for the USDOE under contract DE-AC05-00OR22725U.S.

References

1. Barrera E, Palomar Pardavé M, Batina N, González I (2000) *J Electrochem Soc* 147(5):1787
2. Pfeifer F, Raddeloff C (1980) *J Magn Magn Mater* 19:190
3. Yu RH, Basu S, Zhang Y, Xiao JQ (1999) *J Appl Phys* 85:6034
4. Li L (1996) *J Appl Phys* 79:4578
5. Major RV, Samadian V (1989) *J Mater Eng* 11(1):27
6. Yu RH, Basu S, Zhang Y, Parvizi-Majidi A, Xiao JQ (1999) *J Appl Phys* 85:6655
7. Kakuno EM, Mosca DH, Mazzaro I, Mattoso N, Schreiner WH, Gomes MAB (1997) *J Electrochem Soc* 144(9):3222
8. Fontana RE (1995) *IEEE Trans Magn* MAG-31:2579
9. Grochowski E, Scranton RA, Croll I (1994) In: Romankiw LT, Herman DA Jr (eds) *Magnetic materials, processes, and devices III*, vol PV 94-6. The Electrochemical Society Proceedings Series, Pennington, NJ, p 3
10. Liao SH (1990) *IEEE Trans Magn* MAG-26:328
11. Croll IM (1980) *Advances in X-ray analysis*, vol 4. Plenum Press, New York, p 151
12. Croll IM, May BA (1987) In: Romanikiw LT, Turner DR (eds) *Electrodeposition technology, theory and practice*, vol PV 87-17. The Electrochemical Society Proceeding Series, Pennington, NJ, p 295
13. Brossared L (1991) *Mater Chem Phys* 27:235
14. Cui CQ, Jiang SP, Tseung ACC (1991) *J Electrochem Soc* 138:1001
15. Nishizawa T, Ishida K (1986) *Met Prog* 129(2):57
16. Yu RH, Basu S, Ren L, Zhang Y, Parvizi-Majidi A, Unruh KM, Xiao JQ (2000) *IEEE Trans Magn* 36(5):3388
17. Bozorth RM (1991) *Ferromagnetism*. IEEE, New York
18. Ashby JA, Flower HM, Rawling RD (1977) *Met Sci* 11:91
19. Pitt CD, Rawling RD (1981) *Met Sci* 15:369
20. Yu RH, Zhu J (2005) *J Appl Phys* 97:53905